AIMS Materials Science, 4(1): 194-208.
DOI: 10.3934/matersci.2017.1.194
Received: 02 November 2016
Accepted: 19 January 2017
Published: 24 January 2017

http://www.aimspress.com/journal/Materials

Research article

CVD-graphene growth on different polycrystalline transition metals

M. P. Lavin-Lopez [1,*], L. Sanchez-Silva [2], J. L. Valverde [2], and A. Romero [2]

[1] Graphenano S.L., Calle Pablo Casals 13. Yecla, Murcia, 30510, Spain
[2] Department of Chemical Engineering, University of Castilla-La Mancha, Avenida Camilo Jose Cela 12, Ciudad Real, 13071, Spain

* **Correspondence:** Email: pradolavin@graphenano.com; Tel: +34-926-295-300, ext. 96322.

Abstract: The chemical vapor deposition (CVD) graphene growth on two polycrystalline transition metals (Ni and Cu) was investigated in detail using Raman spectroscopy and optical microscopy as a way to synthesize graphene of the highest quality (i.e. uniform growth of monolayer graphene), which is considered a key issue for electronic devices. Key CVD process parameters (reaction temperature, CH_4/H_2 flow rate ratio, total flow of gases (CH_4+H_2), reaction time) were optimized for both metals in order to obtain the highest graphene uniformity and quality. The conclusions previously reported in literature about the performance of low and high carbon solubility metals in the synthesis of graphene and their associated reaction mechanisms, i.e. *surface deposition* and *precipitation on cooling*, respectively, was not corroborated by the results obtained in this work. Under the optimal reaction conditions, a large percentage of monolayer graphene was obtained over the Ni foil since the carbon saturation was not complete, allowing carbon atoms to be stored in the bulk metal, which could diffuse forming high quality monolayer graphene at the surface. However, under the optimal reaction conditions, the formation of a non-uniform mixture of few layers and multilayer graphene on the Cu foil was related to the presence of an excess of active carbon atoms on the Cu surface.

Keywords: CVD-graphene; carbon solubility; carbon diffusion; thickness; monolayer; copper; nickel; polycrystalline metal

1. Introduction

Graphene is a two dimensional (2D) material of sp^2-bonded carbon atoms with hexagonal structure [1,2]. Two different strategies can be follow to synthesize graphene: *Top Down* strategy in

which graphene is grown by separation or exfoliation of graphite and, *Bottom-Up* strategy in which graphene is grown over a substrate using a carbonaceous gas source [3]. Among all *Bottom-Up* synthesis methods, Chemical Vapor Deposition (CVD) stands out due to its advantage of producing large area of high quality graphene [4,5]. CVD synthesis process consists of a chemical reaction in which a carbonaceous gas source is introduced into a hot reactor. At high temperatures, the hydrocarbon precursor decomposes to carbon radicals forming a graphene layer over the metal substrate. The metal works not only as a catalyst but also determines the growth mechanism of the graphene, which affects considerably the graphene quality, which is related with the type of graphene (multilayer, few layers, bilayer, monolayer) deposited over the sample [6]. In this way, different transition metals can be used as catalysts, such as Ni, Co, Pd, Ru or Cu [7,8,9], being the latter the most widely used. Regarding the carbon solubility, copper shows a low solubility [10] whereas other transitions metals, such as nickel or iron, have higher carbon solubility [11,12]. Depending on the carbon solubility, the graphene-growth mechanism will be different. The *Self-limited Surface Deposition* process appears over transition metals with low carbon solubility (e.g.: Cu, Au) [13] whereas the *Surface Segregation* one occurs over transition metals presenting high carbon solubility (e.g.: Ni, Co, Pt), [14].

In this manuscript, the synthesis of CVD-graphene over both high (Ni) and low (Cu) carbon solubility (polycrystalline) transition metals is reported. In order to study the influence of the metal carbon solubility over the growth and quality of the graphene synthesized, key CVD process parameters such as reaction temperature, CH_4/H_2 flow rate ratio and total flow of gases (at different reaction times) were modified and the properties of resulting materials were compared. Thus, all efforts were aimed at reducing the number of graphene layers over the metal substrate by consequently increasing the graphene quality, which is quantified by a "thickness value". Graphene obtained with both types of metals are compared by considering not only the thermodynamic of metal carbon solubility and, therefore, the growth model proposed for each transition metal, but also aspects such as metal carbon saturation.

2. Materials and Method

2.1. Materials

Polycrystalline copper and nickel foils (2.5 × 4 cm) with a thickness of 25 μm and a purity grade of 99.99% were purchase from GOODFELLOW. Methane, nitrogen and hydrogen with a purity grade of 99.5%, 99.999% and 99.999%, respectively, were provided by PRAXAIR.

2.2. Method

CVD-graphene synthesis was carried out at atmospheric pressure in a quartz tube reactor heated by a furnace. Nickel and copper foils, which act as catalysts, were placed in a quartz boat inside the reactor. In general, four different steps can be distinguished in CVD graphene synthesis (Figure 1): 1) *Heating step:* The furnace was heated at 10 ºC/min until 900 ºC (reduction temperature), under N_2 (inert gas) and H_2 (reduction gas using to prevent the metal foil oxidation); 2) *Reduction step*: The furnace was kept at the reduction temperature for 45 minutes under N_2 and H_2 atmosphere in order to allow the annealing of the metal sheet. Heating and reduction steps were common for both metals

and the same synthesis conditions were used; 3) *Reaction step:* different reaction temperatures were analyzed by varying it between 900 and 1050 ºC. In this step, the inert gas was turned off, maintaining the flow of reduction gas. As the same time, the reaction gas (CH_4) was turned on. Both the CH_4/H_2 flow rate ratio and the total flow of gases (CH_4+H_2) during the reaction step were adjusted in order to work in the range 0.3–0.05 v/v and, 60–130 Nml/min, respectively. A reaction time ranging from 1 to 40 minutes were also considered. 4) *Cooling step:* The system was cooled down until room temperature at 10 ºC/min by passing the same flow of inert gas used in the heating step through the reactor.

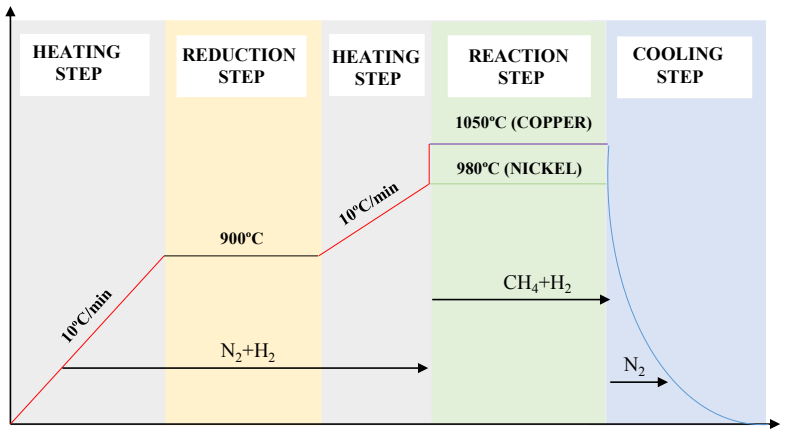

Figure 1. CVD-graphene synthesis parameters.

2.3. Characterization techniques

2.3.1. Raman spectroscopy

A SENTERRA Raman spectrometer with 600 lines per grating and 532 laser wavelength at a very low laser power level (<1mW) was used. Raman is a quick and non-destructive method to characterize graphene based materials.

2.3.2. Optical microscopy

A SENTERRA X50 optical microscope integrated in the Raman spectrometer was used to analyze graphene samples. Several optical microscope images of graphene obtained for each metal catalyst were analyzed. These images showed four different colors directly related to the number of graphene layers present in samples; in other words, each color corresponds to one type of graphene [15,16,17]. Darker orange colors and grain boundaries correspond to *multilayer graphene*, lighter orange colors to *few-layers graphene*, yellow areas to *bilayer graphene* and finally, white zones to *monolayer graphene*.

Figure 2 shows the corresponding Raman spectrum corresponding to each color obtained in the optical microscope images according to the metal catalyst used and, the appearance of the metal foil without graphene. As it could be observed Raman spectroscopy verify that each color corresponds to one type of graphene. In general, lighter colors were associated to less layered graphene and the

darker ones to more layered graphene. In this way, for polycrystalline nickel foils, white and yellow colors corresponds to monolayer and bilayer graphene respectively and, lighter and darker orange correspond to few-layer and multilayer graphene. In the case of polycrystalline copper, the colors are quite different that the one obtained for nickel. Darker orange corresponds to multilayer graphene and, as the color clarified, the number of layer decreased, obtaining the lighter orange for bilayer graphene. Three different peaks can be observed in the typical graphene Raman spectrum. The first one, D peak, is visible around 1350 cm^{-1}, is related to the presence of defects in the sample [18]. Two peaks more, namely G and 2D peak, are located at ~1560 cm^{-1} and 2690 cm^{-1}, respectively. G peak denotes the symmetry-allowed graphite band [18]. 2D peak originates from second order double resonant Raman scattering from zone boundary and is the hall-marks of different numbers of graphene layers [19,20]. This last peak increased from multilayer to monolayer graphene. There are some characteristics Raman parameter, such as, I_D/I_G, I_{2D}/I_G, FWHM (Full Width at Half Maximum) and 2D peak position. The first one corresponds to the amount of defects present in graphene samples. The second one is related to the number of graphene layers and it value increase from multilayer to monolayer graphene. The opposite effect is observed for FWHM parameters, which is calculated as the Raman Shift difference to the half average height of the 2D band and it value decreased from multilayer to monolayer graphene. Finally, 2D peak position shows a characteristic value around 2700 cm^{-1} [21,22,23].

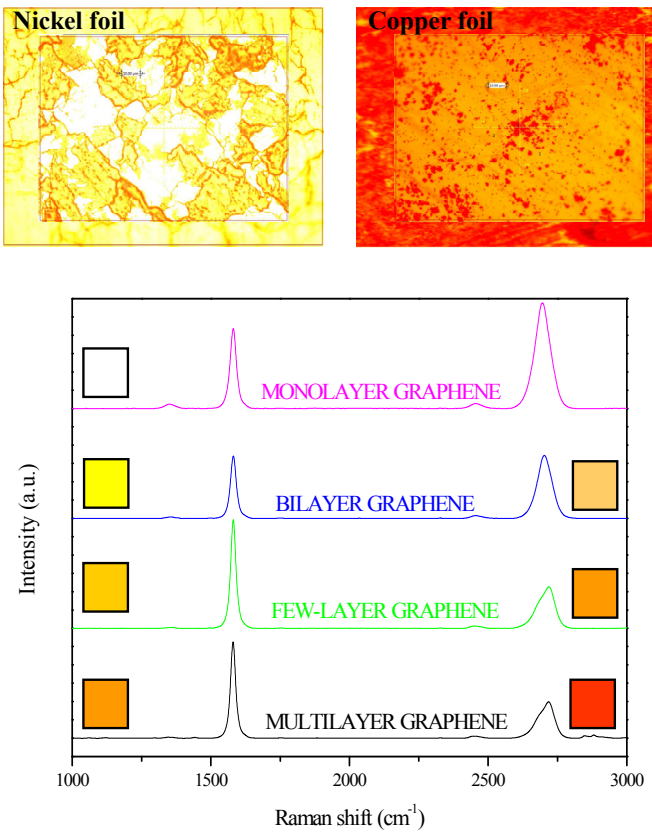

Figure 2. Raman spectroscopy of optical microscope image colors for polycrystalline copper and nickel. Graphene deposited over: right corresponds to polycrystalline nickel foil and left side to polycrystalline copper foil.

2.3.3. Excel-VBA software

In order to analyze the optical microscope images and determine a "thickness value" used to indirectly measure the quality of the graphene samples, an Excel-VBA software was designed. According to the colors appearing in the optical microscope images, and the relationship between these colors and each type of graphene, the software determines the percentage of each type of graphene. Depending on these percentages, the software assigned a "thickness value" between 1 and 1000, corresponding the values 1, 10, 100 and 1000 to a multilayer, few-layers, bilayer or monolayer graphene coverage of the metal foil, respectively. In this sense, the higher the "thickness value", the higher the quality of the sample, i.e., the percentage of monolayer graphene deposited onto the metal foil.

3. Results and Discussion

According to literature, the metal catalyst foil plays an important role on the CVD synthesis of graphene [24,25]. Thus, depending on the carbon solubility of the metal catalyst, two different mechanisms can be distinguished during graphene growth (Figure 3). For low carbon solubility metals, a surface based process called *self-limited surface deposition growth* takes place. Thus, once the hydrocarbon decomposition at high temperatures has taken place, the nucleation and expansion of the carbon atoms to form graphene domains occur [13]. For high carbon solubility metals, a *surface segregation growth mechanism* exists. In this case, the carbon atoms are dissolved into the bulk metal catalyst foil and, when it starts to cool down, these atoms segregate from the bulk to the metal surface forming the graphene sheets [14].

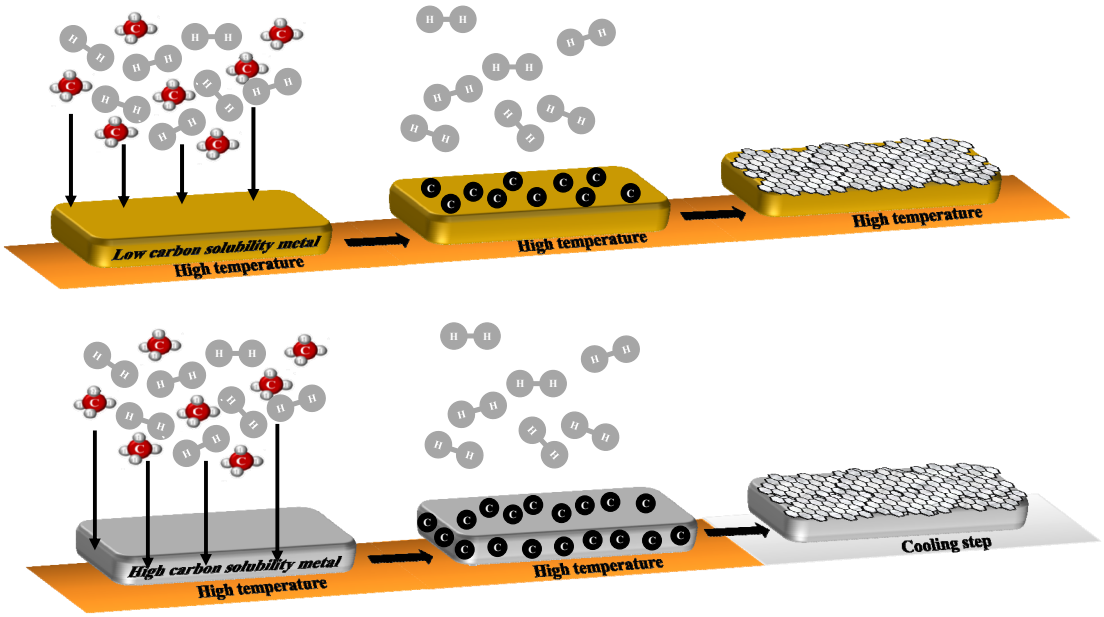

Figure 3. Graphene-growth mechanisms using both high and low carbon solubility metals.

Two different polycrystalline metal substrates with different carbon solubility were used in the present study as catalysts for graphene synthesis: polycrystalline copper as an example of a low

carbon solubility metal, and polycrystalline nickel as an example of a high carbon solubility one. In this study, the use of polycrystalline metals was considered because although they have a rougher surface due to the presence of several grain boundaries, they are much cheaper than the crystalline ones, which is interesting from a large-scale production point of view. However, it is remarkable to note that the synthesis of monolayer graphene over polycrystalline metals is not so favored due to the presence of above mentioned grain boundaries on the metal foil. These grain boundaries are considered as metal impurities and lead to the formation of more layered graphene samples. In addition, they are considered as sites with high chemical activation energy that result in an attraction of more carbon atoms [26,27,28]. On the contrary, those zones without grain boundaries favored the synthesis of less layered graphene, consequently increasing the graphene quality (Figure 4).

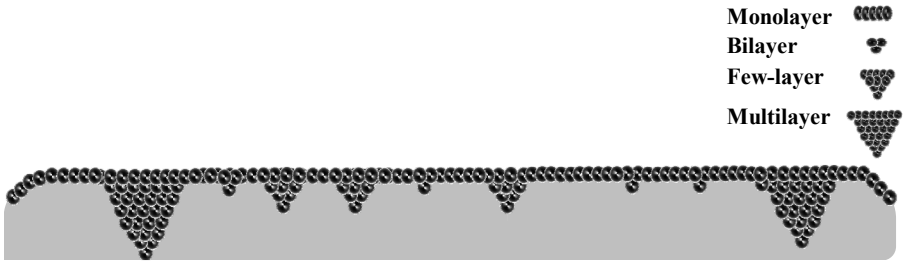

Figure 4. Different types of graphene growth over polycrystalline metal foils.

Reaction temperature is considered a key factor in CVD-graphene synthesis, affecting the homogeneous graphene growth and, consequently, the graphene quality [24,29]. Since CVD is a catalytic process, the carbon precursor dissociation is enhanced at high temperatures. Moreover, grain boundaries dissolution is also favored at high temperatures, which can lead to the synthesis of less layered graphene [30]. Taking into account these two facts, it could be expected high temperatures to lead to the synthesis of high quality graphene. Figure 5 shows for each transition metal and different reaction temperatures the percentage of each type of graphene and the corresponding optical microscope images (including the "thickness value") at the optimum reaction temperature. Obtained results showed an optimum reaction temperature of 1050 and 980 ºC for copper and for nickel, respectively. Both optimal reaction temperatures are within the range reported by other authors, which can vary between 800 and 1100 ºC [15,16]. Summarizing, results showed that a lower reaction temperature was required for the graphene synthesis over the highest carbon solubility metal, Ni, and a higher one for the graphene synthesis over the lowest carbon solubility metal [7]. As reported elsewhere, temperatures close to the metal melting point (1085 ºC in the case of copper) should be used with low carbon solubility metals in order to synthesize high quality graphene [31]. On the other hand, when high solubility metals are used the control the number of graphene layers is not easy because of the precipitation of extra carbon atoms. Ni foils develops a C atoms reservoir within its bulk that precipitate during the cooling step [32]. Consequently, lower reaction temperatures are needed to synthesize high quality graphene because graphene formation really occurs during the cooling step; i.e., extra carbon segregation takes place when the metal foil starts to cool down [14,33].

As observed, no monolayer graphene was observed to cover the copper foil after reaction temperature optimization; i.e., no white areas could be appreciated in optical microscope image,

being the most of the metal foil covered by multilayer graphene (≈ 81%). For nickel, four different colors, and thus, four types of graphene, were however observed. In this case, a low percentage of multilayer graphene after reaction temperature optimization (lesser than 0.87%) was observed, being the most of the sample covered by few-layers (≈ 40%), bilayer (≈ 21%) and monolayer graphene (≈ 37%). As a consequence, nickel catalysts led to a product with a "thickness value" of 397 whereas copper one lead to a product with a "thickness value" of 4.2.

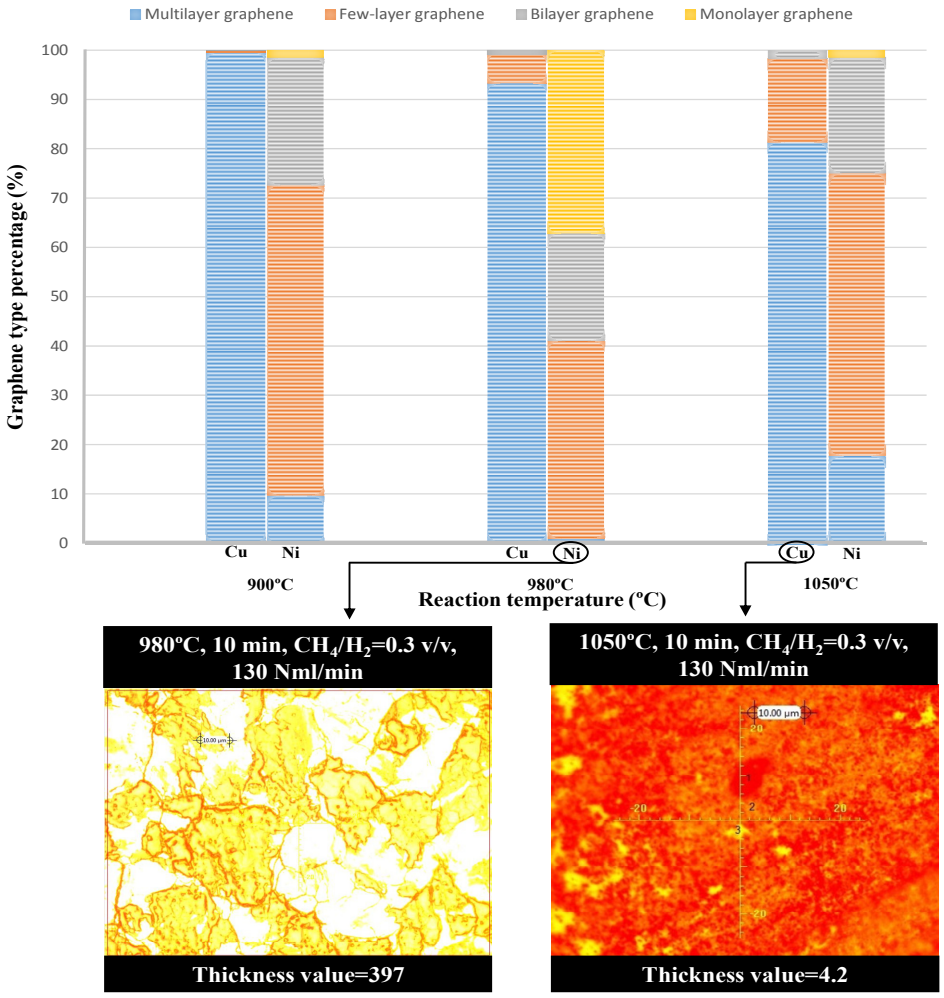

Figure 5. Percentage of each type of graphene at different reaction temperatures, optical microscope images and "thickness values" corresponding to samples synthesized at the optimum temperatures, as a function of the transition metal used as a catalyst.

Carbonaceous source flow determines the concentration of carbon species during CVD-graphene synthesis, also being a key factor to obtain high quality graphene. Two different parameters could be monitored to control the amount of carbon atoms entering into the system during graphene synthesis: the carbonaceous source/hydrogen flow rate ratio, and the total flow of gases (carbonaceous source+hydrogen) during the reaction step.

Figure 6 summarizes the percentage of each type of graphene obtained by varying the CH_4/H_2 flow rate ratio and the optical microscope images (including the "thickness value") corresponding to

the optimum conditions for each transition metal.

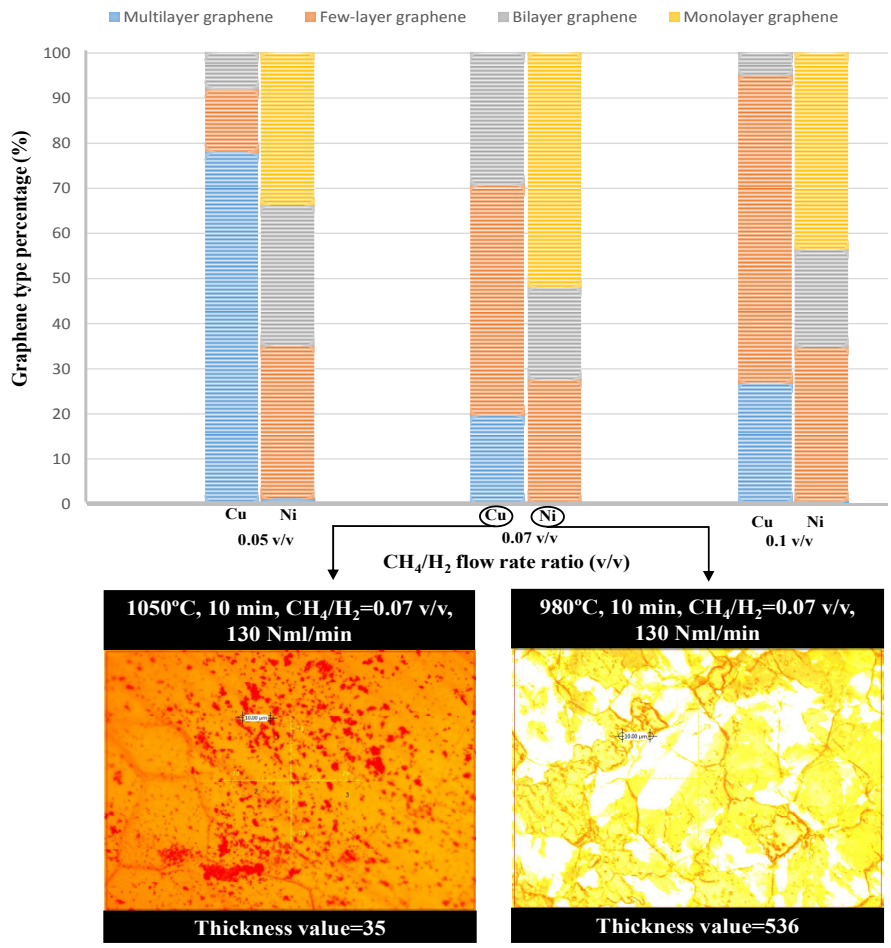

Figure 6. Percentage of each type of graphene at different CH_4/H_2 (v/v), optical microscope images and "thickness values" corresponding to samples synthesized at the optimum CH_4/H_2, as a function of the transition metal used as catalyst.

Regardless the transition metal, the optimum CH_4/H_2 flow rate ratio, allowing to obtain highest quality graphene, was 0.07 (v/v). These results highlight the important role played by the hydrogen in the CVD graphene growth. H_2 helps to clean the metal substrate by removing impurities such as oxides [34]. Also, H_2 plays a more direct role in graphene growth but this fact remains unsolved [35,36]. *Vlassiouk et al.* [35] determined that hydrogen plays a dual role in CVD-graphene synthesis. On the one hand, it acts as cocatalyst in the formation of active surface carbon bonds required for graphene growth. On the other hand, hydrogen controls grain dimension and shape removing the weak C-C bonds.

Significant differences between both transition metals were observed when analyzing the influence of the total flow of gases at different reaction times (Figure 7). Reported studies [15,16,17] showed for both high and low solubility metals agree that the lower the amount of carbon atoms during graphene synthesis, the higher the graphene quality was. The way to get it differs from one metal to another. Thus, higher reaction times (10 min) were needed for a total flow of gases of

60 Nml/min using Cu as catalyst for obtaining graphene with the highest quality. In the case of using Ni as the catalyst, a total flow of 80 Nml/min and a reaction times of 1 min were required.

These results can be explained taking into account the graphene growth mechanism for each metal, which is related to its carbon solubility. Thus, copper, a low carbon solubility metal presenting a *surface deposition* mechanism, required a higher residence time of active carbon atoms than nickel, a high carbon solubility metal presenting a *segregation based* growth mechanism [24]. After optimizing the total flow of gases at different reaction times, graphene sample synthetized by using nickel as catalyst showed a "thickness value" of 810, which meant that around 80% of the sample was covered by monolayer graphene. The best sample synthesized by using copper as catalyst showed a "thickness value" of 59, which meant that both around half of the sample was covered by bilayer graphene and no monolayer graphene was detected.

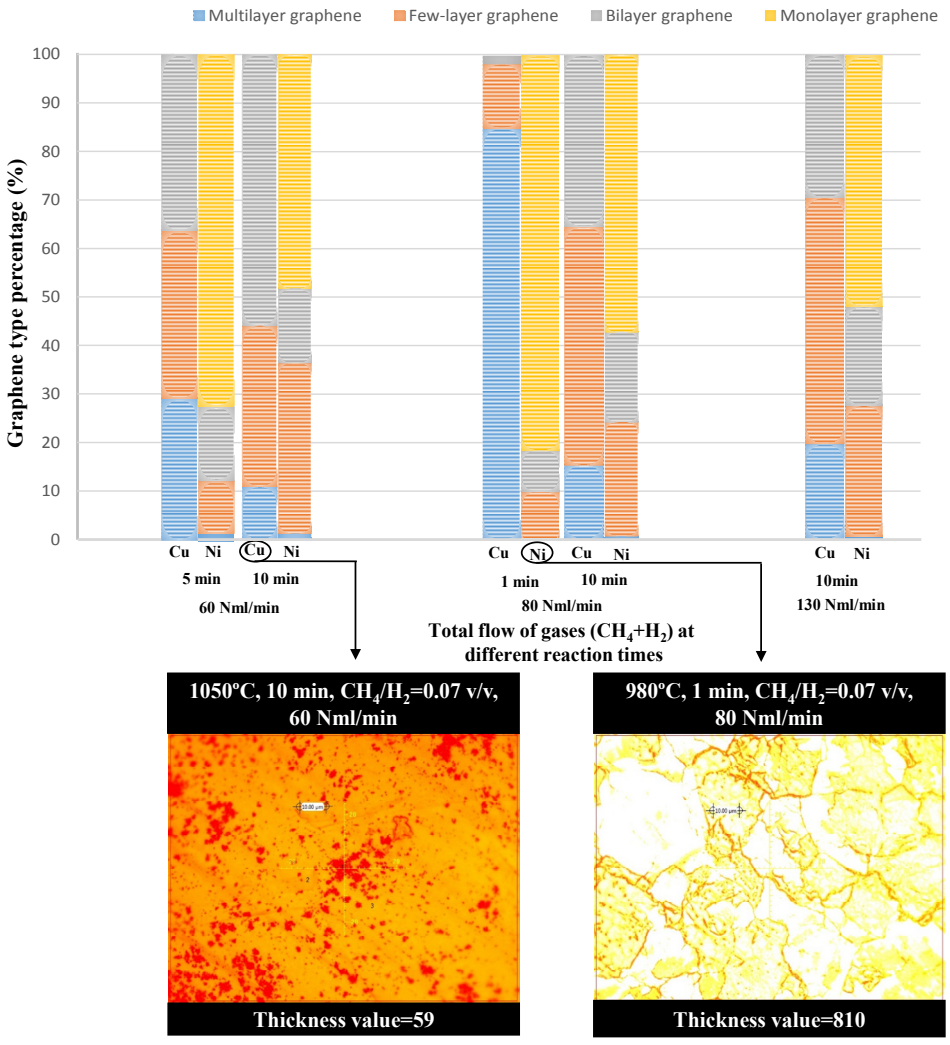

Figure 7. Percentage of each type of graphene at different total flow of gases (CH_4+H_2) and different reaction times, optical microscope images and "thickness values" corresponding to samples synthesized at the optimum total flow of gases, as a function of the transition metal.

These results contradict those reported by other authors. Thus, it has been observed that for a low carbon solubility catalyst, carbon atom supply is self-limited so that monolayer graphene should be formed (once graphene covers the catalyst surface, the catalyst ability for the source gas decomposition plummet) [37]. However, for high carbon solubility catalyst, multilayer graphene is formed during the cooling step due to the solved carbon atoms into the catalyst is segregated at high temperatures, leading to new graphene nucleation at the interface between the first graphene layer and the catalyst [38,39,40]. These claims are not corroborated by our study. In fact, it demonstrates that the growth of monolayer graphene is highly favored in high carbon solubility polycrystalline metals, such as Ni, than in low carbon solubility ones, such as Cu. Thus, simple thermodynamic considerations of carbon solubility are insufficient to explain the graphene growth mechanism in these common catalysts, being necessary take into account other aspects such as catalysts carbon saturation. In this sense, at the conditions at which high quality graphene was obtained by using Ni, this catalyst could not be completely saturated with carbon atoms, allowing that those arriving at the catalyst bulk could diffuse and leading to the formation of monolayer graphene over the surface. Nevertheless, those conditions, at which Ni catalysts could become saturated with carbon atoms (not reached in the present study), should lead to the formation of a more layered graphene sample, since graphene nucleation occurs simultaneously via carbon atoms *solution/segregation* and, via *surface deposition* [40].

For its part, the low solubility of carbon atoms in Cu confines the graphene growth to the Cu surface, which becomes catalytically inactive once it is fully covered with graphene. As commented before, this simple mechanism would limit the growth to a single layer of graphene. However, results obtained in this work using polycrystalline Cu have showed the occurrence of few layer and multilayer graphene which formation is a direct result of the excess of supplied active carbon species [41,42] causing a large saturation of the Cu surface and, as a consequence, a dense nucleation of few-layers and multilayer graphene [43,44,45].

Summarizing, under the used of CVD conditions, nucleation of few layers/bilayer graphene grains is highly preferred rather than the nucleation of monolayer one. Generally speaking, it has been demonstrated that top layers of the multilayer domains always had a smaller size than the underlying layers due to that the supply of active carbon atoms was limited by the growth of graphene layers over the underlying ones (carbonaceous source decomposed just on a Cu surface free of graphene) [46].

Figure 8 shows a representative optical microscope image and a Raman spectrum of each type of graphene deposited on both polycrystalline copper and nickel foils after optimizing the different operational parameters. There are three characteristics peaks in the Raman spectrum of graphene. D peak, which appears around 1350 cm^{-1} and is related to the amount of defects present in graphene sample. The two more intense peaks in the Raman spectrum are G and 2D ones. The first one is associated to the crystallinity of the sample and is located at 1650 cm^{-1}; the second one (2D), which is located around 2700 cm^{-1}, is due to the second order zone boundary phonons and gives information about the number of graphene layers [18,47].

Different Raman parameters, being in all cases characteristics of graphene, were measured [22,26,48]. The ratio of the intensities of D and G peaks (I_D/I_G) presented low values for all the graphene types obtained in both copper and nickel foils, which is related with the presence of low amount of defects. I_{2D}/I_G ratio increased from the multilayer graphene to the monolayer one, being the highest value of this ratio for the monolayer graphene covering the Ni foil. Other remarkable

characteristic parameter derived from the RAMAN spectrum of graphene is the 2D-FWHM (Full Width at Half Maximum), which decreased with the decrease of the number of graphene layers [49,50]. Finally, it was observed that the position of 2D peak positions corresponds to those reported for graphene [47,51,52,53]. Raman spectroscopy parameters shows values according to those obtained in bibliography [54–57].

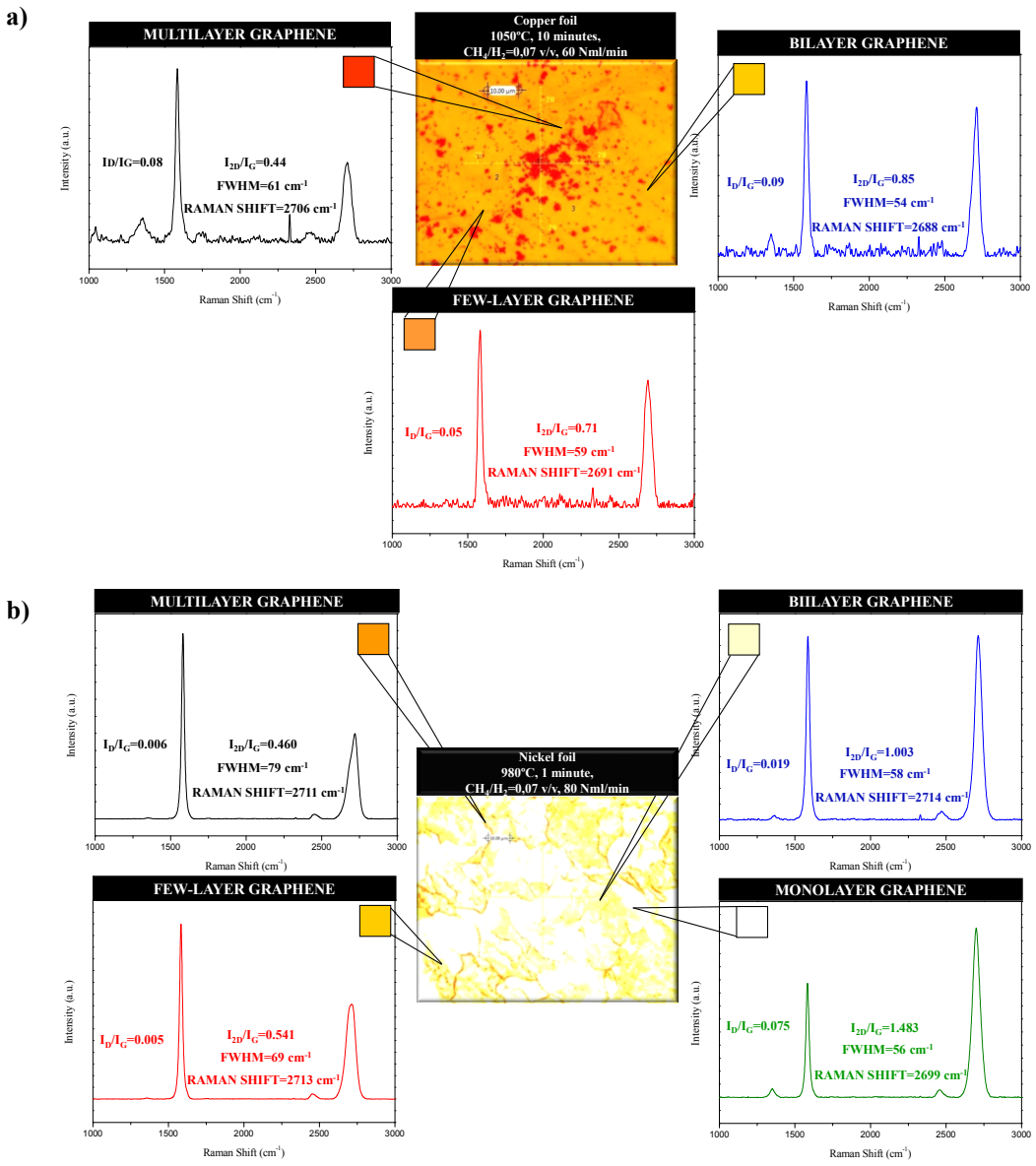

Figure 8. Optical microscope images and Raman spectrum of each type of graphene for samples synthesized at the optimum conditions using polycrystalline copper (a) and nickel (b) foils.

4. Conclusion

The graphene nucleation obtained by catalytic CVD growth was investigated. Transition metal carbon solubility and others issues, such as metal carbon saturation, were related to the results here

obtained. Polycrystalline Cu and Ni were selected as the low and high carbon solubility metals, respectively. Key CVD process parameters (reaction temperature, CH_4/H_2 flow rate ratio, total flow of gases (CH_4+H_2), reaction time) were optimized for both metals in order to obtain the highest graphene uniformity and quality. The conclusions previously reported in literature about the performance of low and high carbon solubility metals in the synthesis of graphene and their associated reaction mechanisms, i.e. *surface deposition* and *precipitation on cooling*, respectively, was not corroborated by the results obtained in this work. The large percentage of monolayer graphene obtained by using Ni foil has been associated to carbon saturation of the metal. Thus, under the selected reaction conditions (980 ºC, CH_4/H_2 = 0.07 v/v, 80 Nml (CH_4+H_2)/min, 1 minute), the carbon saturation was not completely reached. This way, carbon atoms stored into the bulk metal could diffuse forming high quality monolayer graphene over the surface. For its part, under the selected CVD reaction conditions (1050 ºC, CH_4/H_2 = 0.07 v/v, 60 Nml (CH_4+H_2)/min, 10 minutes), the formation of a non-uniform mixture of few layers, bilayer and multilayer graphene on the Cu foil has been related to the presence of an excess of active carbon atoms on the Cu surface.

Conflict of Interest

All authors declare on conflict of interest in this paper.

References

1. Geim A K, Novoselov K S (2007) The rise of graphene. *Nat Mater* 6: 183–191.
2. Chen X, Zhang L, Chen S (2015) Large area CVD growth of graphene. *Synth Met* 210: 95–108.
3. Bhuyan MSA, Uddin MN, Islam MM, et al. (2016) Synthesis of graphene. *Int Nano Lett* 6: 65.
4. Wang Y, Chen X, Zhong Y, et al. (2009) Large area, continuous, few-layered graphene as anodes in organic photovoltaic devices. *Appl Phys Lett* 95: 063302.
5. Dervishi E, Li Z, Watanabe F, et al. (2009) Large-scale graphene production by RF-cCVD method. *Chem Commun,* 4061–4063.
6. Zhang Y, Zhang L, Zhou C (2013) Review of chemical vapor deposition of graphene and related applications. *Acc Chem Res* 46: 2329–2339.
7. Cabrero-Vilatela A, Weatherup RS, Braeuninger-Weimer P, et al. (2016) Towards a general growth model for graphene CVD on transition metal catalysts. *Nanoscale* 8: 2149–2158.
8. Zhang X, Li H, Ding F (2014) Self-Assembly of Carbon Atoms on Transition Metal Surfaces—Chemical Vapor Deposition Growth Mechanism of Graphene. *Adv Mater* 26: 5488–5495.
9. Losurdo M, Giangregorio MM, Capezzuto P, et al. (2011) Graphene CVD growth on copper and nickel: Role of hydrogen in kinetics and structure. *Phys Chem Chem Phys* 13: 20836–20843.
10. López GA, Mittemeijer EJ (2004) The solubility of C in solid Cu. *Scripta Mater* 51: 1–5.
11. Xue Y, Wu B, Guo Y, et al. (2011) Synthesis of large-area, few-layer graphene on iron foil by chemical vapor deposition. *Nano Res* 4: 1208–1214.
12. Chen X, Zhang L, Chen S (2015) Large area CVD growth of graphene. *Synth Met* 210: 95–108.
13. Zhao P, Kumamoto A, Kim S, et al. (2013) Self-Limiting Chemical Vapor Deposition Growth of Monolayer Graphene from Ethanol. *J Phys Chem C* 117: 10755–10763.

14. Yu Q, Lian J, Siriponglert S, et al. (2008) Graphene segregated on Ni surfaces and transferred to insulators. *Appl Phys Lett* 93: 113103.
15. Lavin-Lopez MP, Valverde JL, Cuevas MC, et al. (2014) Synthesis and characterization of graphene: Influence of synthesis variables. *Phys Chem Chem Phys* 16: 2962–2970.
16. Lavin-Lopez MP, Valverde JL, Ruiz-Enrique MI, et al. (2015) Thickness control of graphene deposited over polycrystalline nickel. *New J Chem* 39: 4414–4423.
17. Lavin-Lopez MP, Valverde JL, Sanchez-Silva L, et al. (2016) Influence of the Total Gas Flow at Different Reaction Times for CVD-Graphene Synthesis on Polycrystalline Nickel. *J Nanomater* 2016: 9.
18. Wall M (2012) Raman spectroscopy optimizes graphene characterization. *Adv Mater Processes* 170: 35–38.
19. Suk JW, Kitt A, Magnuson CW, et al. (2011) Transfer of CVD-grown monolayer graphene onto arbitrary substrates. *ACS Nano* 5: 6916–6924.
20. Reina A, Jia X, Ho J, et al. (2009) Large area, few-layer graphene films on arbitrary substrates by chemical vapor deposition. *Nano Lett* 9: 30–35.
21. Lee S, Lee K, Zhong Z (2010) Wafer scale homogeneous bilayer graphene films by chemical vapor deposition. *Nano Lett* 10: 4702–4707.
22. Lee D, Lee K, Jeong S, et al. (2012) Process optimization for synthesis of high-quality graphene films by low-pressure chemical vapor deposition. *Jpn J Appl Phys* 51.
23. Chen S, Cai W, Piner RD, et al. (2011) Synthesis and characterization of large-area graphene and graphite films on commercial Cu-Ni alloy foils. *Nano Lett* 11: 3519–3525.
24. Muñoz R, Gómez-Aleixandre C (2013) Review of CVD synthesis of graphene. *Chem Vap Deposition* 19: 297–322.
25. Seah CM, Chai SP, Mohamed AR (2014) Mechanisms of graphene growth by chemical vapour deposition on transition metals. *Carbon* 70: 1–21.
26. Liu W, Li H, Xu C, et al. (2011) Synthesis of high-quality monolayer and bilayer graphene on copper using chemical vapor deposition. *Carbon* 49: 4122–4130.
27. Li X, Magnuson CW, Venugopal A, et al. (2010) Graphene films with large domain size by a two-step chemical vapor deposition process. *Nano Lett* 10: 4328–4334.
28. Wang YM, Cheng S, Wei QM, et al. (2004) Effects of annealing and impurities on tensile properties of electrodeposited nanocrystalline Ni. *Scripta Mater* 51: 1023–1028.
29. Shen Y, Lua AC (2013) A facile method for the large-scale continuous synthesis of graphene sheets using a novel catalyst. *Sci Rep* 3: 3037–3042.
30. Verguts K, Vermeulen B, Vrancken N, et al. (2016) Epitaxial Al2O3(0001)/Cu(111) Template Development for CVD Graphene Growth. *J Phys Chem C* 120: 297–304.
31. Vlassiouk I, Smirnov S, Regmi M, et al. (2013) Graphene nucleation density on copper: Fundamental role of background pressure. *J Phys Chem C* 117: 18919–18926.
32. Liu W, Chung CH, Miao CQ, et al. (2010) Chemical vapor deposition of large area few layer graphene on Si catalyzed with nickel films. *Thin Solid Films* 518: S128–S132.
33. Wan D, Lin T, Bi H, et al. (2012) Autonomously controlled homogenous growth of wafer-sized high-quality graphene via a smart Janus substrate. *Adv Funct Mater* 22: 1033–1039.
34. Mattevi C, Kim H, Chhowalla M (2011) A review of chemical vapour deposition of graphene on copper. *J Mater Chem* 21: 3324–3334.

35. Vlassiouk I, Regmi M, Fulvio P, et al. (2011) Role of hydrogen in chemical vapor deposition growth of large single-crystal graphene. *ACS Nano* 5: 6069–6076.
36. Zhang Y, Li Z, Kim P, et al. (2012) Anisotropic hydrogen etching of chemical vapor deposited graphene. *ACS Nano* 6: 126–132.
37. Li X, Cai W, Colombo L, et al. (2009) Evolution of graphene growth on Ni and Cu by carbon isotope labeling. *Nano Lett* 9: 4268–4272.
38. Takahashi K, Yamada K, Kato H, et al. (2012) In situ scanning electron microscopy of graphene growth on polycrystalline Ni substrate. *Surf Sci* 606: 728–732.
39. Genki O, Hiroki H, Nanao N, et al. (2012) Macroscopic Single-Domain Graphene Growth on Polycrystalline Nickel Surface. *Appl Phys Express* 5: 035501.
40. Nakahara H, Fujita S, Minato T, et al. (2016) In-Situ RHEED Study on Graphene Growth During Chemical Vapor Deposition. *e-J Surf Sci Nanotechnol* 14: 39–42.
41. Robertson AW, Warner JH (2011) Hexagonal Single Crystal Domains of Few-Layer Graphene on Copper Foils. *Nano Lett* 11: 1182–1189.
42. Yao Y, Li Z, Lin Z, et al. (2011) Controlled Growth of Multilayer, Few-Layer, and Single-Layer Graphene on Metal Substrates. *J Phys Chem C* 115: 5232–5238.
43. Kasap S, Khaksaran H, Celik S, et al. (2015) Controlled growth of large area multilayer graphene on copper by chemical vapour deposition. *Phys Chem Chem Phys* 17: 23081–23087.
44. Van Tu N, Huu Doan L, Van Chuc N, et al. (2013) Synthesis of multi-layer graphene films on copper tape by atmospheric pressure chemical vapor deposition method. *Adv Nat Sci Nanosci Nanotechnol* 4: 035012.
45. Shi Y, Wang D, Zhang J, et al. (2015) Synthesis of multilayer graphene films on copper by modified chemical vapor deposition. *Mater Manuf Process* 30: 711–716.
46. Wu W, Yu Q, Peng P, et al. (2012) Control of thickness uniformity and grain size in graphene films for transparent conductive electrodes. *Nanotechnology* 23.
47.Ferrari AC, Meyer JC, Scardaci V, et al. (2006) Raman spectrum of graphene and graphene layers. *Phys Rev Lett* 97: 187401.
48. Li X, Cai W, An J, et al. (2009) Large-area synthesis of high-quality and uniform graphene films on copper foils. *Science* 324: 1312–1314.
49. Jeong-Yuan H, Chun-Chiang K, Li-Chyong C, et al. (2010) Correlating defect density with carrier mobility in large-scaled graphene films: Raman spectral signatures for the estimation of defect density. *Nanotechnology* 21: 465705.
50. Bointon TH, Barnes MD, Russo S, et al. (2015) High Quality Monolayer Graphene Synthesized by Resistive Heating Cold Wall Chemical Vapor Deposition. *Adv Mater* 27: 4200–4206.
51. Ferrari AC (2007) Raman spectroscopy of graphene and graphite: Disorder, electron-phonon coupling, doping and nonadiabatic effects. *Solid State Commun* 143: 47–57.
52. Nemanich RJ, Solin SA (1979) First- and second-order Raman scattering from finite-size crystals of graphite. *Phys Rev B* 20: 392–401.
53. Calizo I, Teweldebrhan D, Bao W, et al. (2008) Spectroscopic Raman nanometrology of graphene and graphene multilayers on arbitrary substrates. *J Phys* 109: 5.
54. Zhang Y, Gao T, Gao Y, et al. (2011) Defect-like structures of graphene on copper foils for strain relief investigated by high-resolution scanning tunneling microscopy. *ACS Nano* 5: 4014–4022.
55. Nie S, Wofford JM, Bartelt NC, et al. (2011) Origin of the mosaicity in graphene grown on Cu(111). *Phys Rev B Condens Matter* 84: 155425.

56. Rybin MG, Pozharov AS, Obraztsova ED (2010) Control of number of graphene layers grown by chemical vapor deposition. *Phys Status Solidi C* 7: 2785–2788.
57. Liang C, Wang W, Li T, et al. (2012) *Optimization on the synthesis of large-area single-crystal graphene domains by chemical vapor deposition on copper foils*. Xi'an.

AIMS Press

© 2017 M. P. Lavin-Lopez, et al., licensee AIMS Press. This is an open access article distributed under the terms of the Creative Commons Attribution License (http://creativecommons.org/licenses/by/4.0)